New Journal of Physics
The open-access journal for physics

Molecular vibrational cooling by optical pumping with shaped femtosecond pulses

D Sofikitis[1], S Weber[2], A Fioretti[1], R Horchani[1], M Allegrini[1,3], B Chatel[2], D Comparat[1,4] and P Pillet[1]

[1] Laboratoire Aimé Cotton, CNRS, Université Paris-Sud, Bât. 505, 91405 Orsay, France
[2] Laboratoire Collisions, Agrégats, Réactivité (UMR 5589, CNRS—Université Paul Sabatier Toulouse 3), IRSAMC, Toulouse, France
[3] CNISM, Dipartimento di Fisica, Università di Pisa, Largo Pontecorvo, 3 56127 Pisa, Italy
E-mail: daniel.comparat@lac.u-psud.fr

New Journal of Physics **11** (2009) 055037 (17pp)
Received 3 January 2009
Published 14 May 2009
Online at http://www.njp.org/
doi:10.1088/1367-2630/11/5/055037

Abstract. Some of us have recently reported (Viteau *et al* 2008 *Science* **321** 232–4) vibrational cooling of translationally cold Cs_2 molecules into the lowest vibrational level $v = 0$ of the singlet $X^1\Sigma_g$ ground electronic state. Starting from a sample of cold molecules produced in a collection of vibrational levels of the ground state, our method was based on repeated optical pumping by laser light with a spectrum broad enough to excite all populated vibrational levels but frequency-limited in such a way to eliminate transitions from $v = 0$ level, in which molecules accumulate. In this paper, this method is generalized to accumulate molecules into an arbitrary selected 'target' vibrational level. It is implemented by using ultrashort pulse shaping techniques based on liquid crystal spatial light modulator. In particular, a large fraction of the initially present molecules is transferred into a selected vibrational level such as $v = 1$, 2 and 7. Limitations of the method as well as the possible extension to rotational cooling are also discussed.

[4] Author to whom any correspondence should be addressed.

Contents

1. Introduction

The manipulation of atomic or molecular quantum dynamics and the availability of robust and selective methods of executing population transfer in quantum systems are essential for a variety of fields. We could mention precision spectroscopy, quantum computing, control of molecular dynamics and chemical reactions, biophotonics, nanoscience or production of cold molecules [2]–[5]. In particular, the important activities developed in the cold molecule domain through precise control of both internal and external degrees of freedom of a molecule is expected to lead to significant advances in collision dynamics of chemical reactions, molecular spectroscopy, molecular clocks, fundamental test in physics, controlled photo-chemistry studies and also in quantum computation with the use of polar molecules [6]–[11]. Several theoretical approaches have been proposed to control the internal degrees of freedom of a cold molecule such as the use of an external cavity to favor spontaneous emission toward the lowest ro-vibrational level [12] or the controlled interplay of coherent laser fields and spontaneous emission through quantum interferences between different transitions [13]–[16]. Finally, the use of a tailored incoherent broadband light source for internal cooling of molecule has been suggested [17, 18].

During the last two decades many results including coherent control [19]–[21], compression of optical pulses [22] and optical communications [23] have been obtained by the use of arbitrarily shaped optical waveforms. Most of these works were spurred by technological breakthroughs. These pulse shaping techniques have been reviewed in detail [24]. Due to their ultrashort duration, femtosecond pulses are not easily shaped in the time domain. Thanks to the Fourier transformation, the common way to synthesize them is in the spectral domain. The most usual device for both high fidelity and wide flexibility of shapes involves a pair of diffraction gratings and lenses arranged in a zero-dispersion line [25] with a pulse shaping mask at the Fourier plane. In this paper, this technique will be used to improve the vibrational cooling of molecules using amplitude shaping only.

Some of us have recently published an experimental realization of the vibrational cooling based on optical pumping using a train of several identical weak femtosecond laser pulses [1]. Cs_2 molecules initially formed via photoassociation of cold Cs atoms in several vibrational levels, v, of the electronic ground state were redistributed in the ground state via a few electronic excitation–spontaneous emission cycles by applying a femtosecond broadband laser. The laser pulses were shaped to remove the excitation frequency band of the $v = 0$ level, preventing excitation from that state and leading to efficient accumulation in the lowest vibrational level of the singlet electronic state.

Here, using the flexibility of femtosecond pulse shaping techniques [24], this incoherent population pumping method is extended in order to accumulate molecules into other single selected vibrational levels than the sole $v = 0$ one. The outlook of this paper is as follows: we first recall the principle for transferring populations from several energy eigenstates into the lowest vibrational level. We then briefly describe our experimental apparatus and its main parts: the magneto-optical trap (MOT), where the cold molecules are produced and the pulse shaping apparatus based on a liquid crystal spatial light modulator (SLM) placed in the Fourier plane of a highly dispersive 4f line [26]. Then, we report our new experimental result: the selective vibrational cooling of the molecules into one given vibrational level, on demand. Examples are reported for $v = 0$, 1, 2 and 7. In order to improve the efficiency of the optical pumping, we experimentally investigate in more detail the cooling into $v = 1$. Finally, perspectives for very large band vibrational cooling and for rotational cooling are briefly theoretically addressed.

2. Broadband laser cooling of the molecular vibration

2.1. Optical pumping

The main idea, in the optical pumping, as performed in [1], is to use a broadband laser tuned to the transitions between the different vibrational levels, which we label v_X and v_B, belonging, respectively, to the singlet-ground-state $X^1\Sigma_g$, hereafter simply referred as X, and to an electronically excited state, the $B^1\Pi_u$ state of the Cs_2 system, hereafter referred as B. The goal is to start from a given vibrational distribution of v_X values and to transfer it into a single target v_X level. The absorption–spontaneous emission cycles lead, through optical pumping, to a redistribution of the vibrational population into the ground state according to the scheme:

$$Cs_2(v_X) + h\nu_{las} \longrightarrow Cs_2(v_B) \longrightarrow Cs_2(v'_X) + h\nu_{em}, \tag{1}$$

where $h\nu_{las}$ and $h\nu_{em}$ are the energies of the laser and of the spontaneously emitted photons, respectively. The broadband character of the laser permits repetition of the pumping process from multiple vibrational v_X levels. By removing the laser frequencies corresponding to the excitation of a selected v_X level, we make it impossible to pump molecules out of this level, thus making v_X a dark state. As time progresses a series of absorption–spontaneous emission cycles described by equation (1) leads to an accumulation of the molecules in the v_X level.

In the experiment with cold cesium dimers reported in [1], the starting given vibrational distribution was $v_X = 1$–10, the target level was $v_X = 0$, the broadband laser was a Ti : sapphire femtosecond mode-locked laser (standard deviation–gaussian bandwidth 54 cm^{-1}, average intensity of 50 mW cm^{-2}) and the shaping was a simple cut of the blue part of the laser spectrum, which otherwise would have been able to excite the $v_X = 0$ level. In the work presented here, we extend this incoherent depopulation pumping method by using a high resolution pulse shaper. The results are described in the following sections.

2.2. Cold molecule production and pulse shaping

As in the work presented in [1], the cold molecule formation is achieved in a Cs vapor-loaded MOT via photoassociation, where two atoms resonantly absorb a photon to create a molecule in an excited electronic state that decay into stable deeply bound vibrational levels of the singlet molecular ground X state. Photoassociation is achieved using a cw Ti : sapphire laser (intensity 300 W cm^{-2}) pumped by an argon-ion laser.

The stable molecules are then ionized by resonantly enhanced multiphoton ionization (REMPI) with the excited $C^1\Pi_u$ molecular state as the intermediate state. The REMPI detection uses a pulsed dye laser (wavenumber $\sim$16 000 cm^{-1}, spectral bandwidth 0.3 cm^{-1}) pumped by the second harmonic of a pulsed Nd : YAG laser (repetition rate 10 Hz, duration 7 ns). The formed Cs_2^+ ions are detected using a pair of microchannel plates through a time-of-flight mass spectrometer. By scanning the REMPI laser wavelength, the experimental spectrum already presented in [1] and visible in figure 2(d) is monitored. The observed lines represent transitions from vibrational ground states $v_X = 1$–7 level to various levels v_C of the C state [27] (a more detailed study of the process is performed in [28]). The present low REMPI resolution does not provide the capability of analyzing the rotational population of the molecules.

In our experiment, the pulse-shaped femtosecond laser, used to achieve vibrational cooling, is provided by a Kerr-lens-mode-locking Ti : sapphire oscillator with a repetition rate of 80 MHz (12.5 ns between subsequent pulse). The central wavelength is 773 nm. The spectral full-width at half-maximum (FWHM) is around 10 nm.

In order to control the optical pumping, the spectrum of this femtosecond laser is shaped by a high resolution pulse shaper [26]. This one is composed of a dual liquid crystal SLM placed in the Fourier plane of a folded zero dispersion line (see figure 1), which allows phase and amplitude modulation [29].

Let us recall some basics: the incoming laser field E_1 is polarized along the x-axis, z being the propagation axis. The liquid crystals are rod-like molecules that have a variable birefringence. They tend to align themselves with an applied electric field. In this set-up, the liquid crystal molecules are aligned along axis at 45° (for the first SLM) and −45° (for the second SLM) in the x–y-plane. The x-polarized contribution of the outcoming field E_2, noted E_{2x}, can be written as

$$E_{2x}(x) = E_1(x) \times \exp\left(\mathrm{i}(\phi_1(x) + \phi_2(x))\right) \cos(\phi_1(x) - \phi_2(x)), \tag{2}$$

where ϕ_1 and ϕ_2 are the voltage-dependent birefringences of the first and the second liquid crystal arrays, respectively. ϕ_1 and ϕ_2 depend on the x value, i.e. on the considered pixel. So by using an output polarizer along the x-axis, the output phase (retardation) and amplitude (attenuation) can be set independently by controlling the sum and the difference of both liquid crystal birefringences, respectively. Moreover, the use of orthogonal polarizations on each liquid crystal limits multiple diffraction [29]. In this present experiment, amplitude-only modulation is used. The liquid crystal (SLM-S640/12) produced by Jenoptik company, possesses 640 pixels and has been described in [30] (stripes of 97 μm × 10 mm separated by gaps of 3 μm). The birefringence of each pixel is controlled by a voltage with a dynamic range of 12 bits. The nonlinear relation between voltage, incident wavelength and birefringence is carefully calibrated [30]. The regions of liquid crystal between the patterned electrodes cannot be controlled and are referred to as gaps. In these gap regions, the liquid crystals behave in a first approximation as though there were zero applied voltage so that the filter for the gap regions is assumed to be constant across the array. This limits

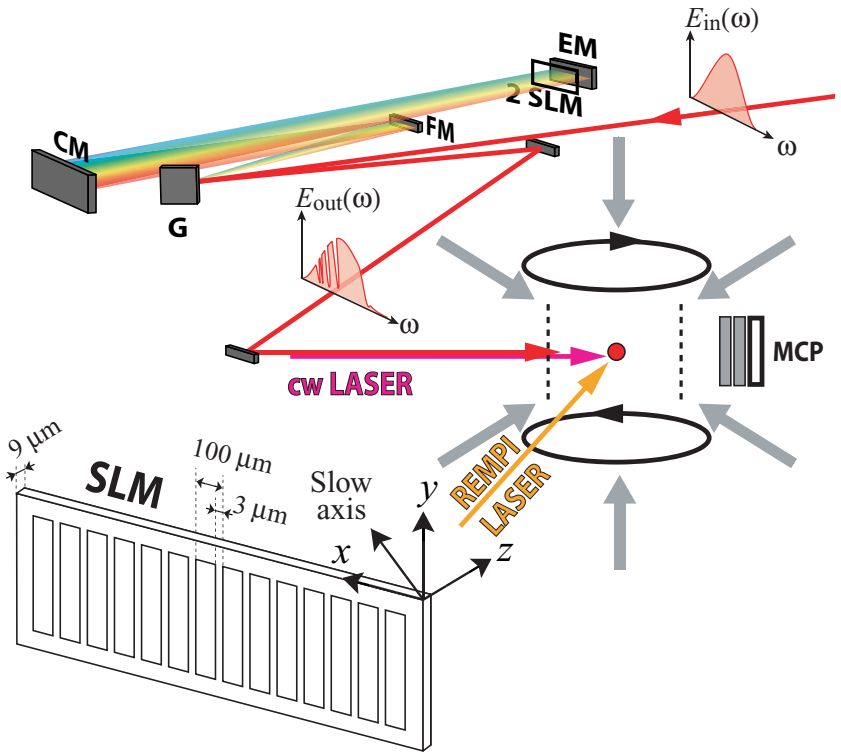

Figure 1. Experimental set-up for the pulse shaper and the cold molecule production and detection. Upper part: folded zero dispersion line, also called the 4f-line. The beam is dispersed by the grating G and then each spectral component is spatially separated and focalized by the cylindrical mirror CM in the Fourier plane. FM is a plane-folded mirror. Both SLMs (detailed in the lower-left side of the figure) are at the Fourier plane. An end mirror EM is placed just after the SLM and the beam goes twice through the folded line. The shaped light is then sent to the cold molecular cloud, which is created by photoassociation (with the cw laser) of an atomic Cs cloud cooled by a standard six beams vapor-loaded MOT. The molecules are then detected using a REMPI ionization laser creating Cs_2^+ ions, which are accelerated by an electric field created with the two grids surrounding the cloud, and monitored using a micro-channel plate (MCP).

the off–on ratio (degree of extinction) of theoretically 20 dB (99% intensity extinction). However, probably due to imperfect experimental polarization, one has measured, using an OCEAN Optics HR 4000 spectrometer, only an off–on ratio of 3% of the light intensity in the worse case. In the simulation of the experiment, this 3% conservative value is the reference.

To avoid chromatic as well as off-axis aberrations, the set-up shown in figure 1 is chosen. The beam is first dispersed by a gold-coated grating with 2000 lines mm^{-1} and then focused in the horizontal plane by a cylindrical mirror with a focal length of 600 mm in the Fourier plane. The two liquid crystal SLMs (64 mm width) are placed in the Fourier plane just behind the end mirror which allows us to fold the line without any misalignment effect thanks to the large Rayleigh length. In this design, the beam passes twice through the dual liquid crystal.

By construction, this setup provides a perfect symmetry of the zero-dispersion line that greatly simplifies the alignment procedure. The central wavelength of the 4f-line is set as 773 nm.

These characteristics provide an average resolution of 0.06 nm pixel^{-1} corresponding to a spectral width of 38 nm. This spectral width is large enough to transmit the spectral pedestal width of our laser source (FWHM of 10 nm). The sagittal beam FWHM in the Fourier plane (57 μm, corresponding to an input beam diameter of 2.3 mm) is roughly set to the width of a pixel, therefore maximizing the resolution of the pulse shaper. Temporal replicas inherent to these liquid crystal devices are not a limitation for this experiment.

The overall transmission in intensity of all of the device is currently 60%, mainly limited by the grating's efficiency, which is enough in the present experiment because one uses an average laser power of only a few milliwatts focused on the molecular cloud with a waist of nearly 500 μm. A similar laser power of 3 mW, corresponding to an intensity of 700 mW cm^{-2}, is used in these simulations.

3. Experimental results

3.1. Vibrational cooling to the vibrational ground state

As already explained, accumulation in a given vibrational level comes from the fact that all the frequencies that could excite molecules decaying in this level during the optical pumping procedure are removed, making it a dark state of the system. The femtosecond laser spectrum needed to realize such a dark state is first theoretically calculated, and then implemented using the pulse shaper. In order to predict the best possible laser spectrum, we have modeled the optical pumping in a very simple way. Using the known X and B potential curves and their rotational constants [31, 32], we calculate the ro-vibrational energy levels as well as the Franck–Condon (FC) factors for the transitions. Because of the very low average laser intensity we are in a perturbative regime. Thus, we could assume that the excitation probability is simply proportional to the laser spectral density at the transition frequencies, to the FC factor, and to the Hönl–London factor. If needed rate equations can be performed, and exactly solved using for instance kinetic Monte Carlo modeling [33], but in our strong perturbative regime, where much less than one photon is absorbed during the excited state lifetime ($\sim$15 ns), we simply assume that all of the population has decayed before sending, 12.5 ns later, another broadband light pulse. Initially, in each simulation, the molecules lie in the levels $v_X = 1$–10, with a distribution measured experimentally in [1] and corresponding to the spectrum (without the femtosecond laser) of figure 2(d).

In the first experiment, presented in figure 2, we use our SLM setup in order to recover the results already presented in [1], where the shaping was simply realized by using a razor blade in the Fourier plane of a 4f-line. Starting from the sample of cold molecules in vibrational levels $v_X = 1$–7 of the ground state, the idea is to use the broadband laser to excite all populated vibrational levels but frequency-limited in such a way to eliminate transitions from $v = 0$ level, in which molecules accumulate. For the cesium dimer, the frequencies that correspond to excitation of the ground vibrational level $v_X = 0$ to any vibrational level of the B potential lie higher than a specific threshold of 13 000 cm^{-1}. Consequently, the required laser shape spectrum is simply the usual laser spectrum truncated at this threshold. The theoretical (assuming a Gaussian shape and a 3% extinction ratio) as well as the experimentally realized spectra are presented in figure 2(b). During the femtosecond excitation step, only a part of the transitions,

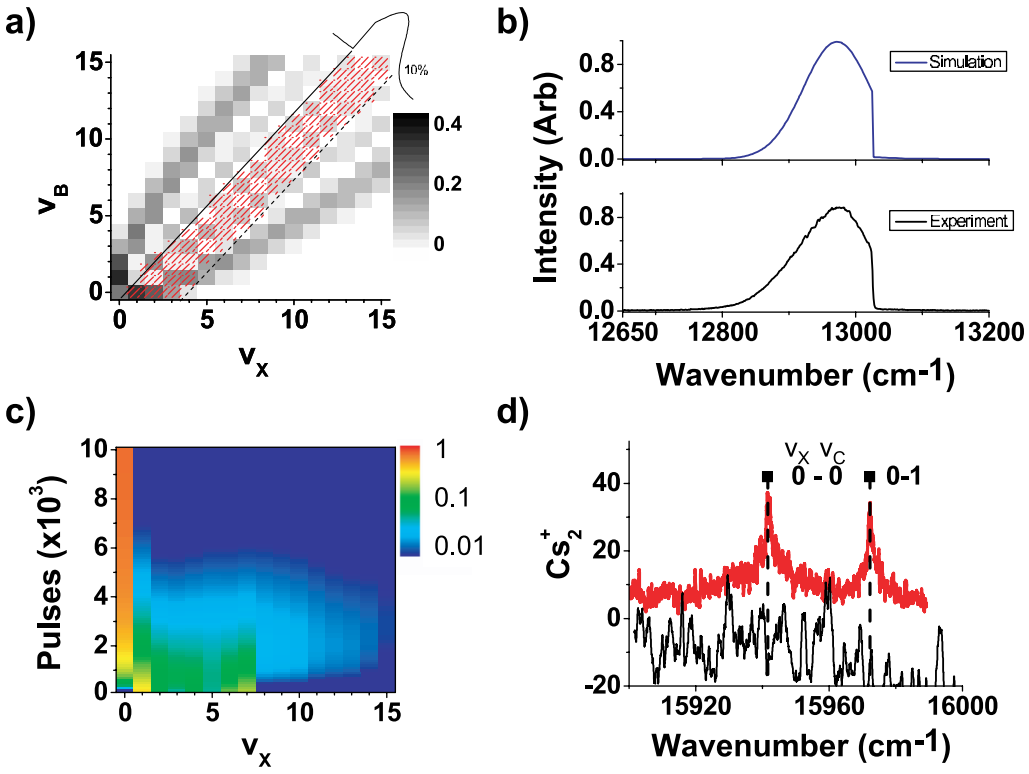

Figure 2. Simulation and experimental results for the transfer in the vibrational ground state. (a) FC coefficients (grey scale) for transition between the X ground state and the B excited state. The hatched (red) area represents the transitions that are excited by the pulse-shaped laser intensity, only transitions with laser intensity more than 10% of maximum intensity are shown. The sharp cut in the laser spectrum is represented by a solid line. (b) The shaped pulse used for the simulation (upper part) and in the experimental one (lower part). (c) Results of the simulation of the vibrational cooling where the (log scale) color level indicates molecular population. The accumulated population in each v_X level is plotted as a function of the number of femtosecond pulses. The femtosecond laser pulses occur every 12.5 ns. After 10^4 pulses the population in the $v_X = 0$ level is 70%. (d) REMPI molecular ion spectrum with the shaped femtosecond pulses (in red). This is the signature of $v_X = 0$ molecules because only transitions from $v_X = 0$ to $v_C = 0$ and $v_C = 1$ are present in the spectrum. The spectrum (in black, with an offset of -40 for clarity) without femtosecond pulses [1], indicating the presence of molecules in several low vibrational levels, is reported for reference.

between the v_X and v_B vibrational levels of the ground X and the excited B electronic states, can occur since the available laser frequencies are limited. In order to understand the basics of the optical pumping process, we represent (in hatched red) in figure 2(a) the transitions that can be excited by the pulse-shaped laser and (in grey) the FC factors for the transitions between the v_X and the v_B vibrational states. The (grey) FC parabola is useful to study the spontaneous decay of an excited molecule, whereas the hatched red part is useful to study the

laser excitation. The sharp energy cut in the laser spectrum is represented by a solid line in this v_X, v_B graph because the energy varies almost linearly with the vibrational quantum number due to the small anharmonicity in each of the X and B potential curves. As an example, let us follow the optical pumping of a molecule initially in the $v_X = 4$ level: its most probable optical pumping walk is first to be excited into $v_B = 1$ (stronger FC factor in the hatched area) then to decay in $v_X = 0$ (stronger FC factor), where no more excitation is possible (no hatched transition). More generally, the result is given by the complete simulation and is shown in figure 2(c). After the application of 10^4 pulses, 70% of the initial population, spread among several vibrational levels, have been transferred into the sole $v_X = 0$ level. The remaining 30% of the population is transferred to high vibrational levels that are not affected by the femtosecond laser because the possible transitions lie out of the range of frequencies available in the laser pulse we use. With a larger bandwidth laser, the simulation shows that a better efficiency of the process is possible (see section 4).

When applying the shaped femtosecond laser to the cold molecules, the experimental result is shown in figure 2(d), where the detection of the vibrational level populated is done via a 2-photon REMPI scheme at 627 nm (DCM dye laser) via the $C^1\Pi_u$ state. We clearly see strong lines appearing at energies corresponding to $v_X = 0 \rightarrow v_C = 0$, 1 transitions that are missing when the shaped femtosecond pulses are not applied. Due to some instabilities of the detection scheme, it is difficult to quantify the fraction of transferred population, which is theoretically 70%.

3.2. Selective cooling to a single vibrational level

The idea of removing the frequencies that correspond to (all) possible excitations of a particular vibrational level, in order to form a dark state where molecular population can accumulate with optical pumping, can be applied not only to the $v_X = 0$ level. Figure 3 shows the case where the target vibration state is $v_X = 1$, where we have shaped the pulse by removing many transition frequencies between $v_X = 1$ and the B state. The required spectrum and its realization by the pulse shaper are shown in figure 3(b). Several tests have been performed in order to study the effect of the number of pixels (between 1 and 5) used to make the 'holes'. No substantial difference has been shown on the REMPI signal. In all the experiment two neighboring pixels are usually set to zero. This emphasizes that although our pulse shaper has a high resolution, the molecular transitions are narrow enough to be killed by only one 'dark pixel'. The 0.06 nm limited resolution of the pulse shaper does not cause any problem as long as this does not lead to a second 'dark' state in the system, a condition which is easily fulfilled due to the relatively large spectral separation ($\sim$40 cm^{-1}, corresponding to 2.3 nm at 13 000 cm^{-1}) of the lower vibrational levels. In figure 3(b) below, the experimental spectrum is recorded by a spectrometer (Ocean optics HR 4000) with a resolution half the pulse shaper's one.

The simulation, shown in figure 3(c), predicts a total transfer of 53% to the $v_X = 1$ level, value that could be increased up to 67% if a perfect off–on ratio is simulated. Finally, figure 3(d) shows the detected ion spectrum, where frequencies corresponding to $v_X = 1 \rightarrow v_C = 0, 1, 2, 3$ transitions, appear with a strong signal.

The generality of the method is demonstrated in figure 4, where the case for the $v_X = 0$, 1, 2 and 7 target states are presented. For each chosen target v_X, the ionization spectrum contains mainly lines in positions corresponding to transitions from the selected target state to several excited vibrational levels.

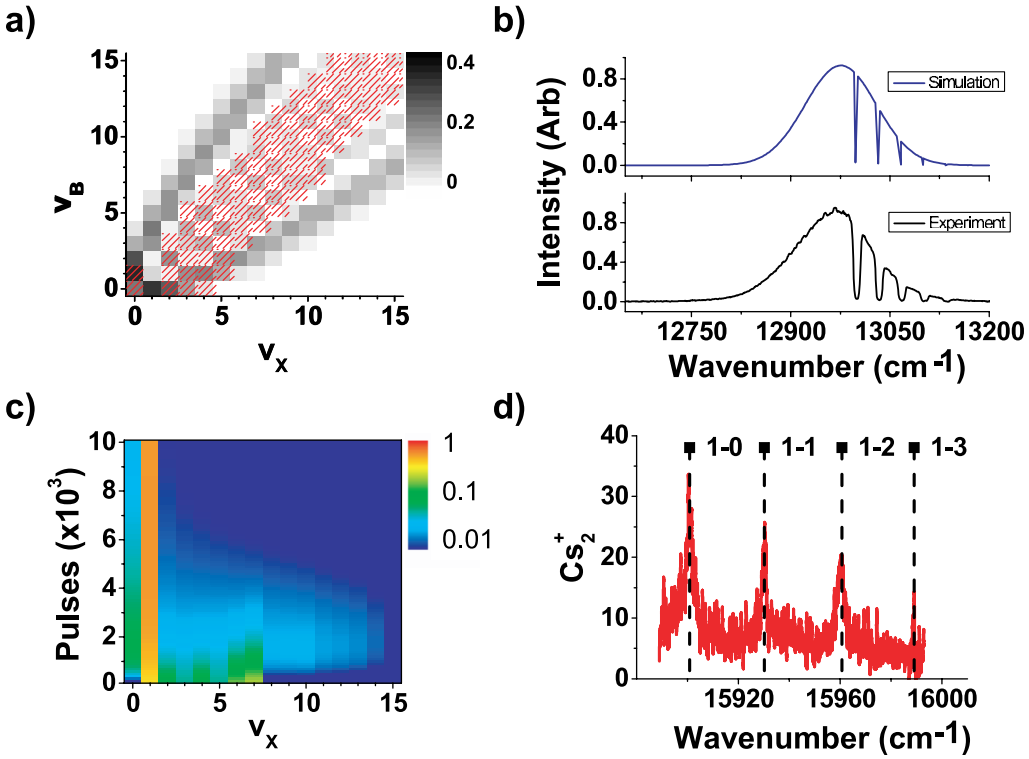

Figure 3. Simulation and experimental results for the transfer in the $v_X = 1$ level. (a) FC coefficients (grey) for transition between the X ground state and the B excited state. The hatched (red) area represents transitions allowed (i.e. having an intensity higher than 10% of the maximum) by the shaped laser pulse: transitions from $v_X = 1$ level, which is now the 'target' state, are completely removed. (b) The shaped pulse used for the simulation (upper part) and in the experiment (lower part). (c) Results of the simulation of the vibrational cooling. The population of the $v_X = 1$ level after 10^4 pulses is 53%. (d) Experimental detection spectrum of molecule (mainly in $v_X = 1$) via two-photon REMPI.

In principle, any vibrational level can be chosen as the target state. The obvious limitation lies upon the available laser bandwidth and upon the initial molecular distribution. The laser has to be strong enough in the vicinity of transitions between the initial states and the target one. For the femtosecond laser used here (bandwidth 55 cm^{-1}), $v_X = 7$ is an extreme choice, a fact that is indicated by a lower signal to noise ratio and the existence of $v_X = 0$, 1 contributions to the signal.

3.3. Better shaping and accumulation analysis

It has been demonstrated that population can be transferred to a desired vibrational level when the frequencies that connect it to any of the excited states used in the optical pumping scheme are removed from the femtosecond pulse. However, the efficiency of such an optical pumping procedure depends on the FC factor, i.e. on the relative position of the electronically excited potential with respect to the ground-state one, on the bandwidth of the femtosecond pulse used and on the extinction ratio of the pulse shaper.

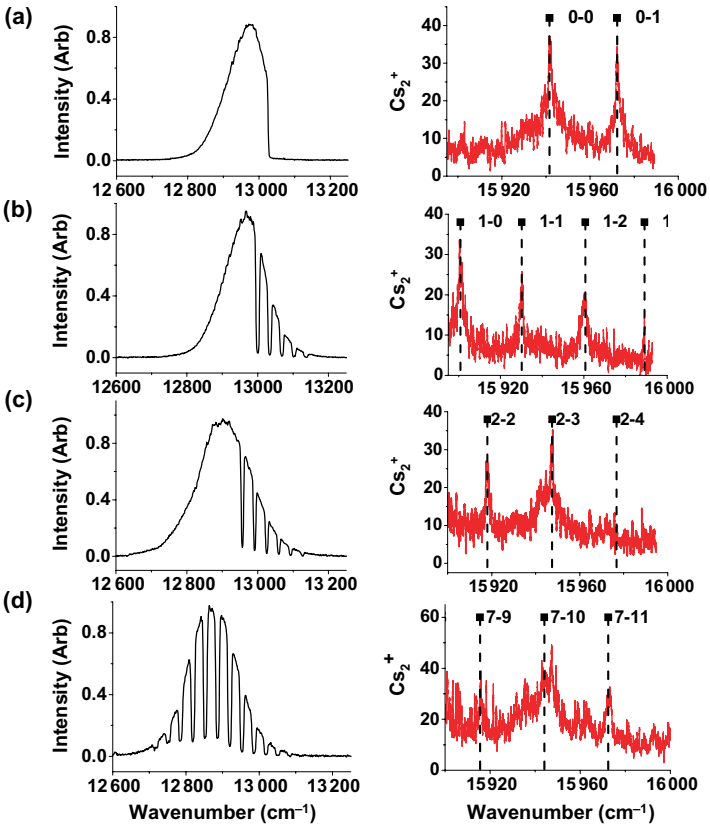

Figure 4. Left part: the experimental pulse spectra used to populate the $v_X = 0$ (a), $v_X = 1$ (b), $v_X = 2$ (c) and $v_X = 7$ (d) levels. Right part: the corresponding experimental ionization spectra. Notice that in spectrum (c) a small signal corresponding to molecules in $v_X = 0$ remains, and that in spectrum (d) molecules in the $v_X = 1$ level also remain.

We would like here to address more complex pulse shaping which could possibly lead to more efficient vibrational cooling, in terms of the number of molecules finally transferred to the desired state, than the one just described. As a particular example we will study the case of a 'comb' of selected laser frequencies chosen in such a way to induce only the transition required to produce efficient optical pumping from the initially populated levels to the target one. Several approaches exist for the choice of such an optimized spectrum but of course, the target state has to remain a dark state and all frequencies resonant to it must be removed. A possible criterion for the choice of the allowed excited states is that their FC coefficients with the target vibrational level should be as high as possible. However, in our case, due to the limited laser bandwidth, it is more important to limit the transfer of population to high vibrational levels that are no longer affected by the femtosecond laser. Therefore, one has chosen to favor excitation in levels that correspond to the 'lower branch' of the FC parabola. With such a choice, once a v_X molecule is excited in this 'lower branch', it will decay either in the same v_X level or in the 'upper branch' of the FC parabola, i.e. in lower vibrational levels than its initial value.

An example is given in figure 5, where the target state is again the $v_X = 1$ level. Using the SLM all laser frequencies are removed from the pulse spectrum, except those that excite

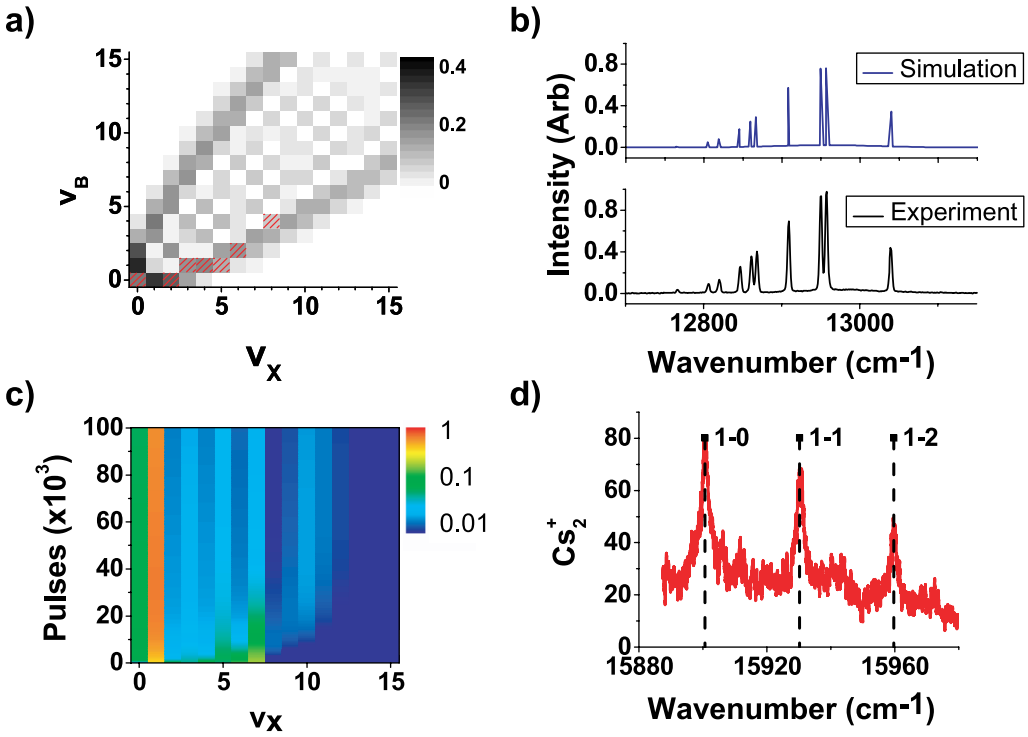

Figure 5. Same as figure 3 but for the transfer in the $v_X = 1$ level with an improved shaping. (a) FC coefficients (grey) for transition between the X ground state and the B excited state. The hatched (red) area represents transitions allowed by the shaped laser pulse: i.e. between $v_X \neq 1$ to v_B levels that decay in levels $v'_X \leqslant v_X$. (b) The shaped pulse used for the simulation (upper part) and in the experiment (lower part). (c) Results of the simulation of the vibrational cooling. The population of the $v_X = 1$ level after 10^5 pulses is 57% which could be increased up to 98% if a perfect off–on ratio is simulated. (d) Experimental detection of (mainly $v_X = 1$) molecules via two-photon REMPI.

the various vibrational levels $v_X \neq 1$ to levels v_B that decay (see equation (1)) in levels $v'_X \leqslant v_X$.

The simulation of the required pulse (shown in figure 5(b) upper part) shown in figure 5(c) predicts a transfer for the 'comb' pulse of 57%, which is better than the 53% of the corresponding 'hole' pulse used in figure 3(c). On the experimental side, the larger signal in figure 5(d) with respect to the corresponding figure 3(d) seems to indicate that the population transfer is indeed, in the 'comb' pulse case, more efficient than using the 'hole' pulse one.

By controlling the number of femtosecond laser pulses with an acousto-optic modulator, we analyzed the time dependence of the optical pumping scheme in figure 6. One has recorded the temporal evolution of the vibrational cooling (as a function of the number of femtosecond pulses) with the use of the pulses shown in figures 3 and 5, compared with the result of the simulation. Here again the behavior is the expected one. If it is difficult in the current experiment to make a precise statement concerning the efficiency of the process, it is clear that, as expected, the optimized 'comb' pulse is slower than the 'hole' one. This is not a general feature but is

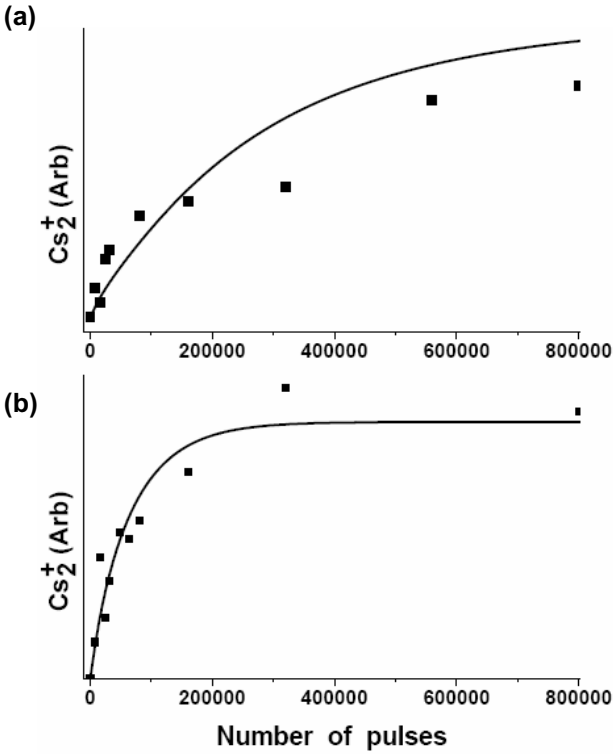

Figure 6. Temporal evolution of the population of the $v_X = 1$ level. (a) With the pulse plotted in figures 5(b) and (b) with the pulse plotted in figure 3(b). The lines correspond to the simulation and the dots to experimental measurements, i.e. to the Cs_2^+ ion signal recorded with the REMPI laser tuned to the transition $v_X = 1$ to $v_B = 0$ at 15 900 cm^{-1}.

simply due in our case to the limited laser bandwidth that limits the ability to excite the 'lower branch' of the FC parabola especially for high vibrational levels.

4. Outlook and perspectives for broadband laser cooling

4.1. Efficient accumulation of population

Due to the limited laser bandwidth and the imperfect extinction ratio of our SLM, the transfer efficiency seems to be limited to roughly 60%. The simulation clearly indicates that both effects are important. Indeed, a three times broader laser, shaped in a similar manner to the previous one (excitation on the lower part of the Condon parabola), would lead to a transfer efficiency toward $v_X = 1$ of 67%. Furthermore, as indicated by figure 7, a perfect off–on ratio would even lead to an almost perfect transfer efficiency (99.4%).

4.2. Rotational cooling

Let us note that for the Cs dimer, the resolution required in order to separate all rotational levels would be of the order of 0.01 cm^{-1} (corresponding to 0.0006 nm), which is difficult to achieve experimentally and beyond the capabilities of the present pulse shaper which has a 0.06 nm

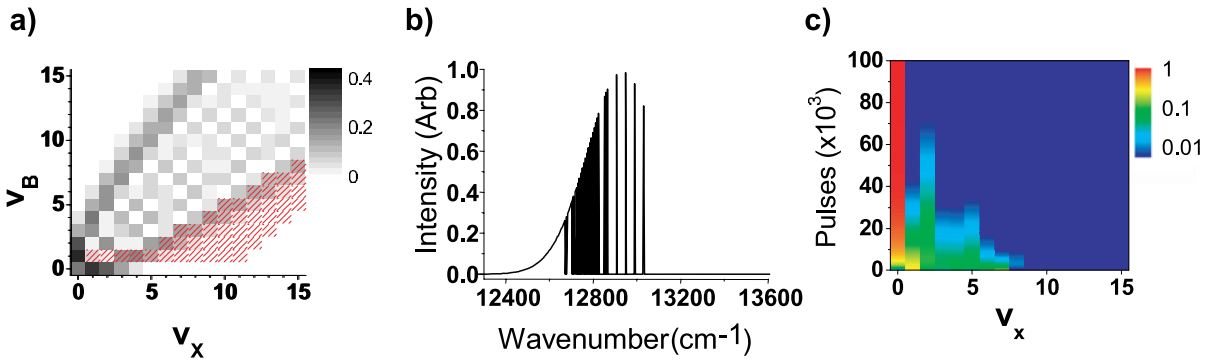

Figure 7. Simulation for the vibrational cooling, similar to figure 5, but with the use of a broader-shaped pulse (but with the same total intensity) and with a perfect off–on extinction ratio. (a) FC coefficients (grey) for transition between the X ground state and the B excited state. The hatched (red) area represents absorption allowed transitions. (b) The shaped pulse used for the simulation. The bandwidth is now three times larger than the one of the previous pulses (165 cm^{-1}). (c) Results of the simulation of the vibrational cooling. The population of the $v_X = 0$ level after 10^5 pulses is 99.4%.

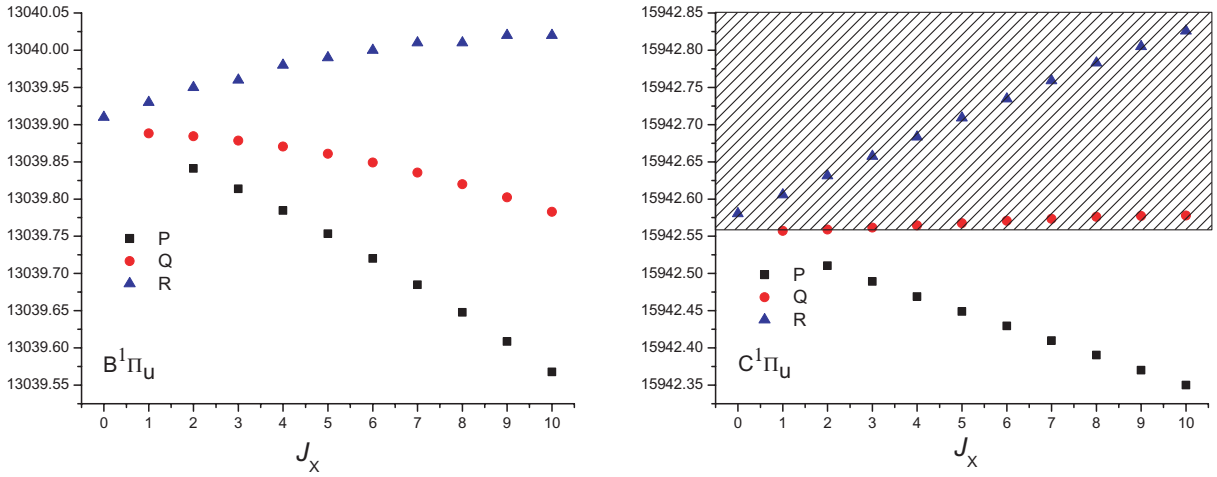

Figure 8. Energy of the different ro-vibrational transitions (for the $\Delta J = 0, \pm 1$ Q R and P branches). (a) $\Delta J = J_B - J_X$ with the B state, (b) $\Delta J = J_C - J_X$ with the C state. The C state permits rotational cooling with a simple laser shaping, which is not possible via the B state due to the energy dependence of the transitions. By removing all frequencies larger than 15 942.557 cm^{-1}, we ensure that $\Delta J = J_C - J_X = -1$ in each excitation step except for the $J_X = 1$ to $J_C = 1$ transition. This way the $J_X = 0$ is the only dark state of the system.

resolution. However, the simulation can be used to answer one important question: can the laser cooling of the vibration to be extended to the rotation of the molecules? As is done with vibration, we could think that an optimized shaping or just a 'cut' could realize a rotational

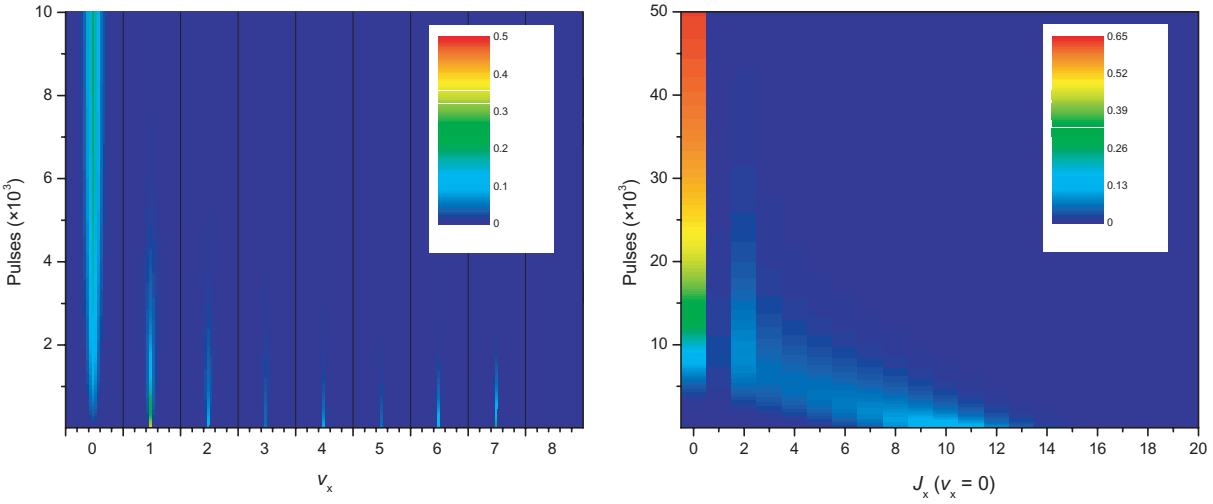

Figure 9. Simulation of the temporal evolution for a ro-vibrational cooling. On the left side, the vibrational cooling to the $v_X = 0$ level, where the cooling is realized as in figure 2 via the state B with all frequencies above 13 000 cm^{-1} suppressed (just below the $v_X = 1$, $v_B = 0$ transition energy). Here the nine first vibrational levels are shown, each of them containing (shown from left to right in order) 21 rotational levels. Initially all population is placed in the $J = 10$ level, a fact that does not affect the validity of the calculation, since the population is redistributed in the rotational levels under the influence of the optical pumping laser. On the right side, the rotational cooling to the $v_X = 0$, $J_X = 0$, that follows this vibrational cooling, is realized via the state C (laser wavelength 15 940.0 cm^{-1}, FWHM laser linewidth 50 cm^{-1}), where all frequencies above 15 942.557 cm^{-1} are suppressed, and with an initial rotational distribution which corresponds to the output of the vibrational cooling step.

cooling. However, we could not totally control the absorption step by an arbitrary shaping due to the selection rules $\Delta J = 0, \pm 1$ so a more detailed study is required.

We would like to demonstrate that rotational cooling is indeed, in principle, feasible by studying the simple possible case of population transfer toward the lowest ro-vibronic state of the Cs_2 molecules, namely $v_X = J_X = 0$ level, where J_X represents the rotational quantum numbers in the X state.

A possibility for laser cooling of the molecular rotation is to shape the laser by removing the frequencies corresponding to the transitions $\Delta J = J_B - J_X = 0, +1$, where J_X and J_B represent the rotational quantum numbers in each level. With such a shaping, absorption–spontaneous emission cycles would indeed lead to a decrease on average of the principal rotation quantum number J_X, i.e. to a laser cooling of the rotation. Figure 8 shows the energies corresponding to the rotational transitions between the vibrational levels $v_X = 0$ and $v_B = 0$.

By analogy with what has been performed for the vibrational cooling realized in figure 2, a simple 'cut' in the laser spectrum could be implemented. By a blue cut of the laser, it is not possible to suppress the transitions $\Delta J = J_B - J_X = 0$ (Q branch). This indicates that this simple 'cut' of the spectrum would not be an efficient way to perform the rotational cooling through the B state. However, rotational cooling through the B state is possible by selecting only the P-branch using a shaper with a very high selectivity.

But for simplicity we shall study another situation where we consider no longer the state, $B^1\Pi_u$, but the state, $C^1\Pi_u$. Figure 8 shows that the transitions $\Delta J = J_C - J_X = 0$ can be easily suppressed by a simple energy cut. Furthermore the high FC value between $v_X = 0$ and $v_C = 0$ ensures that no spurious heating could occur by population transfer to $v_X \neq 0$ levels.

Figure 9 shows the results of a simulation, where the molecules are first vibrationally cooled, as is done in figure 2, i.e. by applying the excitation of the state, $B^1\Pi_u$, then rotationally cooled by considering the excitation of the state $C^1\Pi_u$. Obviously such a scheme would require an external broadband source to excite the X states toward the C one, one could think of a simple broadband diode laser near 627 nm.

5. Conclusion

We have studied experimentally how femtosecond pulse shaping techniques can be used to realize efficient optical pumping of the vibration of cold Cs_2 molecules. We have used only a small part of the possibilities offered by the pulse shaping techniques, namely using them as an intensity spectral modulator for incoherent optical pumping. Using a shaped laser with higher power could open several possibilities demonstrated to coherently transfer population between ro-vibrational levels [13]–[16]. However, the method demonstrated here is based on a light spectrally broad enough to excite a large number of populated vibrational levels and shaped in amplitude such that it eliminates all frequencies that could excite the desire target state v. With an appropriate pulse shaper, we have demonstrated the optical pumping to single vibrational levels such as $v = 0$, 1, 2 and 7. We have also demonstrated the possibility to optimize the pumping method by using convenient pulse shaping in order to excite only the most appropriate vibrational transitions. Rotational cooling can, in principle, be performed in a similar way provided that the laser bandwidth and the experimental ability to shape the laser matches the rotational energy spread.

The efficiency of the optical pumping is mainly limited by the finite laser spectral bandwidth and the imperfect extinction ratio of our SLM. However, the theory indicates that the use of broader sources and better off–on ratio has the possibility to accumulate near 100% of population in one single vibrational level. Therefore, the use of super-continuum source or a simple broadband diode laser in combination with better (no gap) SLM or with mechanical shutters might be interesting for this purpose. This opens the way to use such a source as repumping light in a scheme for laser cooling of molecules [34, 35]. Finally, accumulation of the molecules in an optical trap could lead to the study of collisional processes in order to assess the efficiency of evaporative cooling or to investigate ways for achieving controlled chemistry.

Acknowledgments

This work is supported by the 'Institut Francilien de Recherche sur les Atomes Froids' (IFRAF) and (in Toulouse) by the Agence Nationale de la Recherche (Contract ANR-06-BLAN-0004) and the Del Duca foundation. MA thanks the EC-Network EMALI. We thank Nadia Bouloufa and Olivier Dulieu for providing us with the FC calculations, and Matthieu Viteau and Amodsen Chotia for the previous realization of part of the experimental set-up.

References

[1] Viteau M, Chotia A, Allegrini M, Bouloufa N, Dulieu O, Comparat D and Pillet P 2008 Optical pumping and vibrational cooling of molecules *Science* **321** 232–4

[2] Ye J and Cundiff S T 2005 *Femtosecond Optical Frequency Comb Technology: Principle, Operation and Applications* (New York: Springer)

[3] Shapiro M and Brumer P 2003 *Principles of the Quantum Control of Molecular Processes* (Hoboken, NJ: Wiley-Interscience)

[4] D'Alessandro D 2007 *Introduction to Quantum Control and Dynamics* (Boca Raton, FL: Chapman and Hall)

[5] Rabitz H, de Vivie-Riedle R, Motzkus M and Kompa K 2000 Whither the future of controlling quantum phenomena? *Science* **288** 824–8

[6] Doyle J, Friedrich B, Krems R V and Masnou-Seeuws F 2004 Editorial: Quo vadis, cold molecules? *Eur. Phys. J.* D **31** 149–64

[7] Krems R V 2005 Molecules near absolute zero and external field control of atomic and molecular dynamics *Int. Rev. Phys. Chem.* **24** 99–118

[8] Hutson J M and Soldan P 2006 Molecule formation in ultracold atomic gases *Int. Rev. Phys. Chem.* **25** 497

[9] Dulieu O, Raoult M and Tiemann E 2006 Cold molecules: a chemistry kitchen for physicists? *J. Phys. B: At. Mol. Opt. Phys.* **39** doi: 10.1088/0953-4075/39/19/E01

[10] Krems R V 2008 Cold controlled chemistry *Phys. Chem. Chem. Phys.* **10** 4079

[11] Smith I W M 2008 *Low Temperatures and Cold Molecules* (London: Imperial College Press)

[12] Morigi G, Pinkse P W H, Kowalewski M and de Vivie-Riedle R 2007 Cavity cooling of internal molecular motion *Phys. Rev. Lett.* **99** 073001

[13] Bartana A, Kosloff R and Tannor D J 1993 Laser cooling of molecular internal degrees of freedom by a series of shaped pulses *J. Chem. Phys.* **99** 196–210

[14] Tannor D J, Kosloff R and Bartana A 1999 Laser cooling of internal degrees of freedom of molecules by dynamically trapped states *Faraday Discuss.* **113** 365–83

[15] Bartana A, Kosloff R and Tannor D J 2001 Laser cooling of molecules by dynamically trapped states *Chem. Phys.* **267** 195–207

[16] Schirmer S G 2000 Laser cooling of internal molecular degrees of freedom for vibrationally hot molecules *Phys. Rev.* A **63** 013407

[17] Vogelius I S, Madsen L B and Drewsen M 2002 Blackbody-radiation-assisted laser cooling of molecular ions *Phys. Rev. Lett.* **89** 173003

[18] Vogelius I S, Madsen L B and Drewsen M 2004 Rotational cooling of molecules using lamps *J. Phys. B: At. Mol. Opt. Phys.* **37** 4571–4

[19] Assion A, Baumert T, Bergt M, Brixner T, Kiefer B, Seyfried V, Strehle M and Gerber G 1998 Control of chemical reactions by feedback-optimized phase-shaped femtosecond laser pulses *Science* **282** 919

[20] Monmayrant A, Chatel B and Girard B 2006 Quantum state measurement using coherent transients *Phys. Rev. Lett.* **96** 103002

[21] Herek J L, Wohlleben W, Cogdell R J, Zeidler D and Motzkus M 2002 Quantum control of energy flow in light harvesting *Nature* **417** 533

[22] Efimov A, Moores M D, Mei B, Krause J L, Siders C W and Reitze D H 2000 Minimization of dispersion in an ultrafast chirped pulse amplifier using adaptive learning *Appl. Phys.* B **70** S133

[23] Sardesai H P, Chang C C and Weiner A M 1998 A femtosecond code-division multiple-access communication system test bed *J. Lightwave Technol.* **16** 1953

[24] Weiner A M 2000 Femtosecond pulse shaping using spatial light modulators *Rev. Sci. Instrum.* **71** 1929–60

[25] Martinez O E 1987 3000 times grating compressor with positive group velocity dispersion: application to fiber compensation in 1.3–1.6 μm region *IEEE J. Quantum Electron.* **23** 59

[26] Monmayrant A and Chatel B 2004 A new phase and amplitude high resolution pulse shaper *Rev. Sci. Instrum.* **75** 2668

[27] Raab M, Höning G, Demtröder W and Vidal C R 1982 High resolution laser spectroscopy of Cs_2. II. Doppler-free polarization spectroscopy of the $C^1\Pi_u \rightarrow X^1\Sigma_g^+$ system *J. Chem. Phys.* **76** 4370–86
[28] Viteau M, Chotia A, Allegrini M, Bouloufa N, Dulieu O, Comparat D and Pillet P 2009 Efficient formation of deeply bound ultracold molecules probed by broadband detection *Phys. Rev.* A **79** 021402
[29] Wefers M M and Nelson K A 1995 Analysis of programmable ultrashort waveform generation using liquid-crystal spatial light-modulators *J. Opt. Soc. Am.* B **12** 1343
[30] Stobrawa G, Hacker M, Feurer T, Zeidler D, Motzkus M and Reichel F 2001 A new high-resolution femtosecond pulse shaper *Appl. Phys.* B **72** 627
[31] Weickenmeier W, Diemer U, Wahl M, Raab M, Demtröder W and Müller W 1985 Accurate ground state potential of Cs_2 up to the dissociation limit *J. Chem. Phys.* **82** 5354–63
[32] Diemer U, Duchowicz R, Ertel M, Mehdizadeh E and Demtröder W 1989 Doppler-free polarization spectroscopy of the $B^1\Pi_u$ state of Cs_2 *Chem. Phys. Lett.* **164** 419–26
[33] Chotia A, Viteau M, Vogt T, Comparat D and Pillet P 2008 Kinetic Monte Carlo modeling of dipole blockade in Rydberg excitation experiment *New J. Phys.* **10** 045031
[34] Bahns J T, Stwalley W C and Gould P L 1996 Laser cooling of molecules: a sequential scheme for rotation, translation and vibration *J. Chem. Phys.* **104** 9689–97
[35] di Rosa M D 2004 Laser-cooling molecules *Eur. Phys. J.* D **31** 395–402